Supplemental Figures

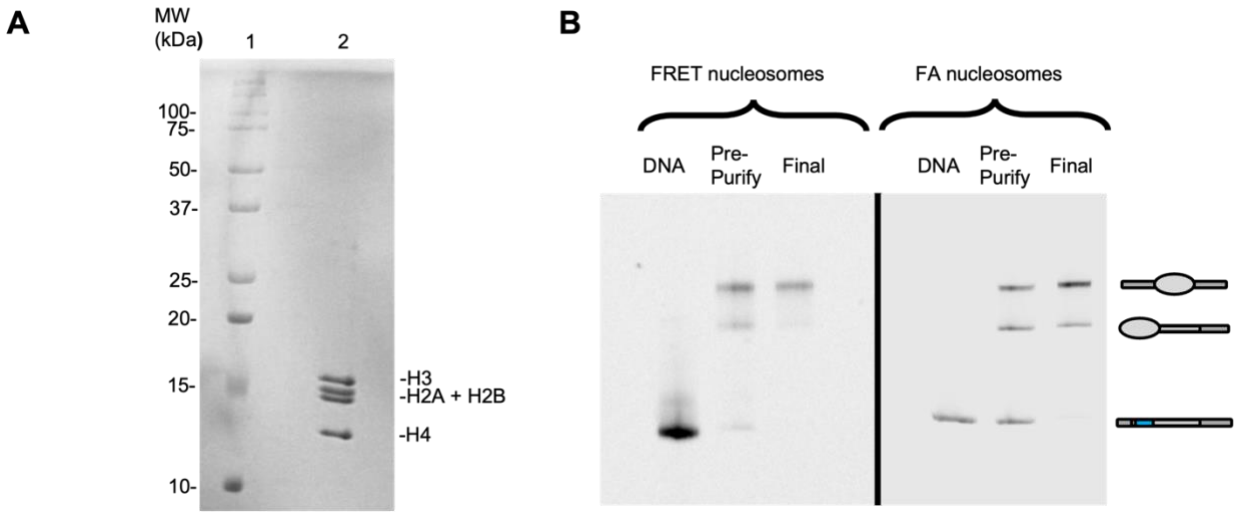

Figure S1. Histone octamer and nucleosome preparations. (A) Purified histone octamer visualized on SDS PAGE gel (lane 2). Lane 1: molecular weight (MW) markers in kDa. (B) Native PAGE analysis of purified nucleosomes. DNA lane contains only DNA used to make nucleosomes. Pre-Purify lane contains nucleosomes before sucrose gradient purification. Final lane contains nucleosomes after sucrose gradient purification. The slower mobility nucleosome band contains center-positioned nucleosomes while the faster mobility nucleosome band contains end-positioned nucleosomes.

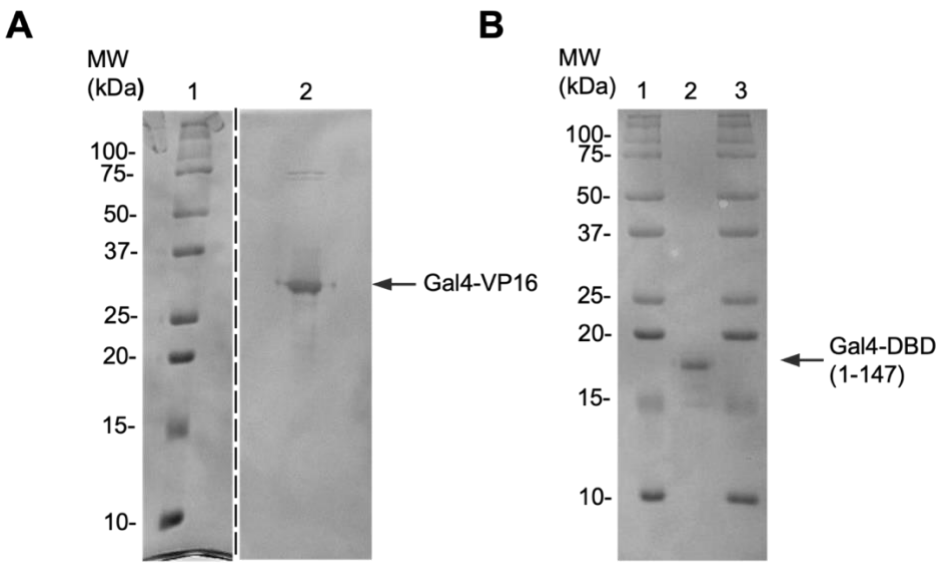

Figure S2. Gal4-VP16 and Gal4-DBD purification. The purified Gal4-VP16 (A) and Gal4-DBD (from amino acid 1 to 147) (B) proteins were visualized on SDS PAGE gel by Coomassie blue staining, Lane 1 in (A) and lanes 1 and 3 in (B): molecular weight (MW) markers in kDa.

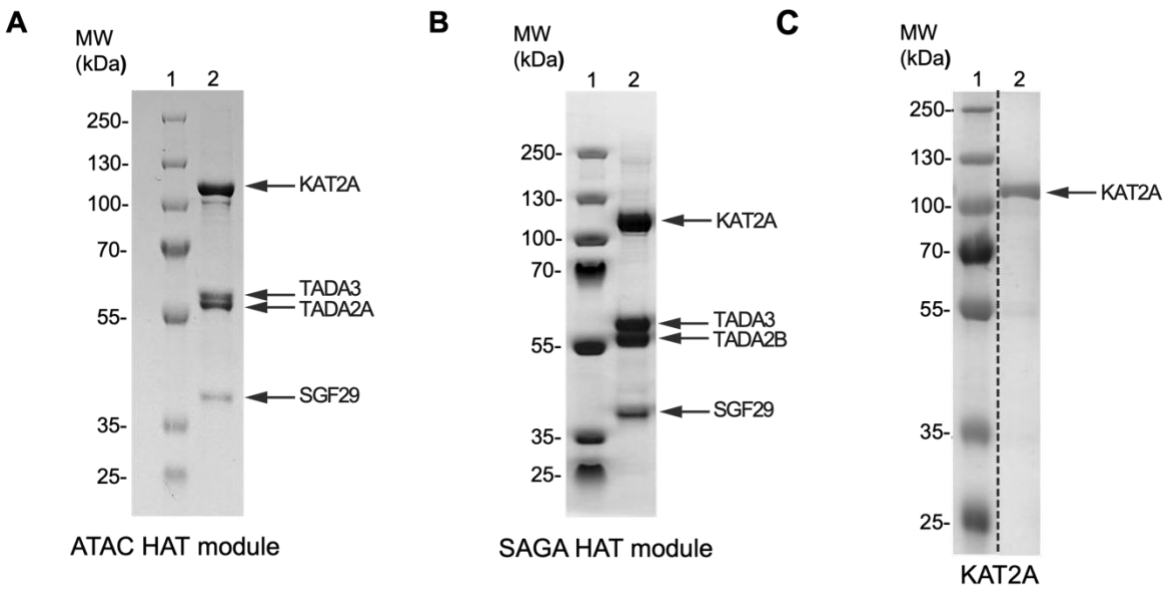

Figure S3. ATAC and SAGA HAT module purifications. (A) Highly purified $ATAC_{HAT}$ (A) and $SAGA_{HAT}$ (B) were visualized on SDS PAGE gel by Coomassie blue staining. Lane 1 in (A) and (B) molecular weight (MW) markers in kDa. (C) Purified Flag-KAT2A (lane 2).

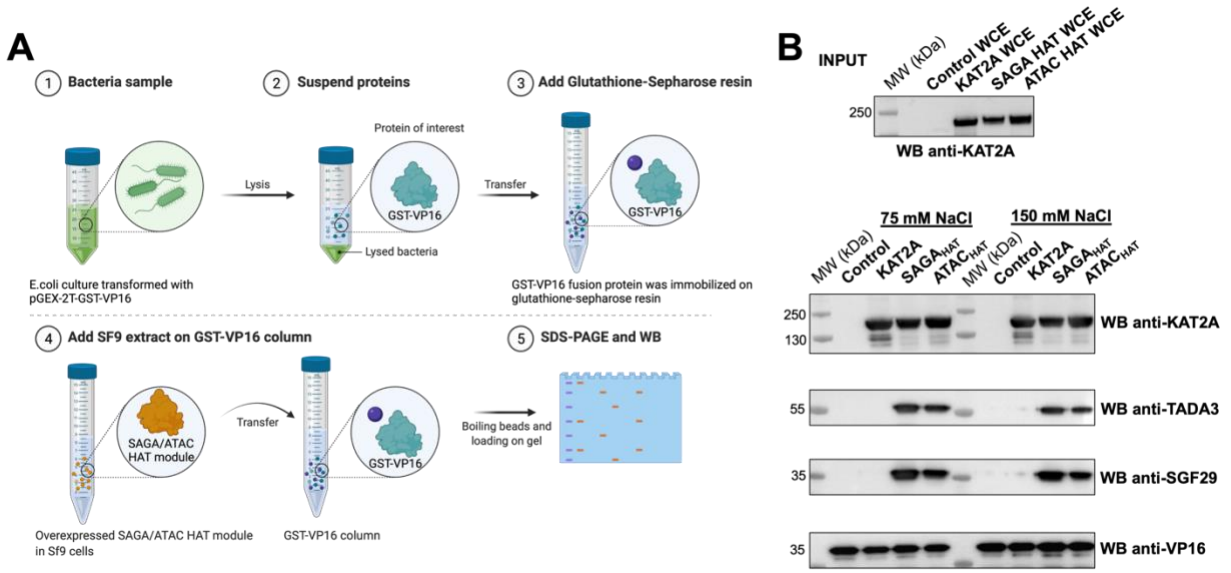

Figure S4. Specific binding of the HAT module of SAGA and ATAC complexes to VP16-AD. (A) Schematic representation of experimental workflow. (B) Western blot analysis of the elutes from the GST-VP16 column, using SF9 whole cell extracts (WCE) where recombinant KAT2A protein, $SAGA_{HAT}$ or $ATAC_{HAT}$ modules were overexpressed by baculovirus overexpression system in Sf9 cells, separately. Upper panel indicates overexpression levels of KAT2A in each whole cell extracts. Lower panels indicate the presence KAT2A and HAT module subunits in 10% elutions from the GST-VP16 column in the presence of either 75 mM NaCl or 150 mM NaCl. Molecular weight (MW) markers in kDa are indicated. The indicated proteins were detected by Western blot assays (WB) using antibodies raised against the indicated proteins.

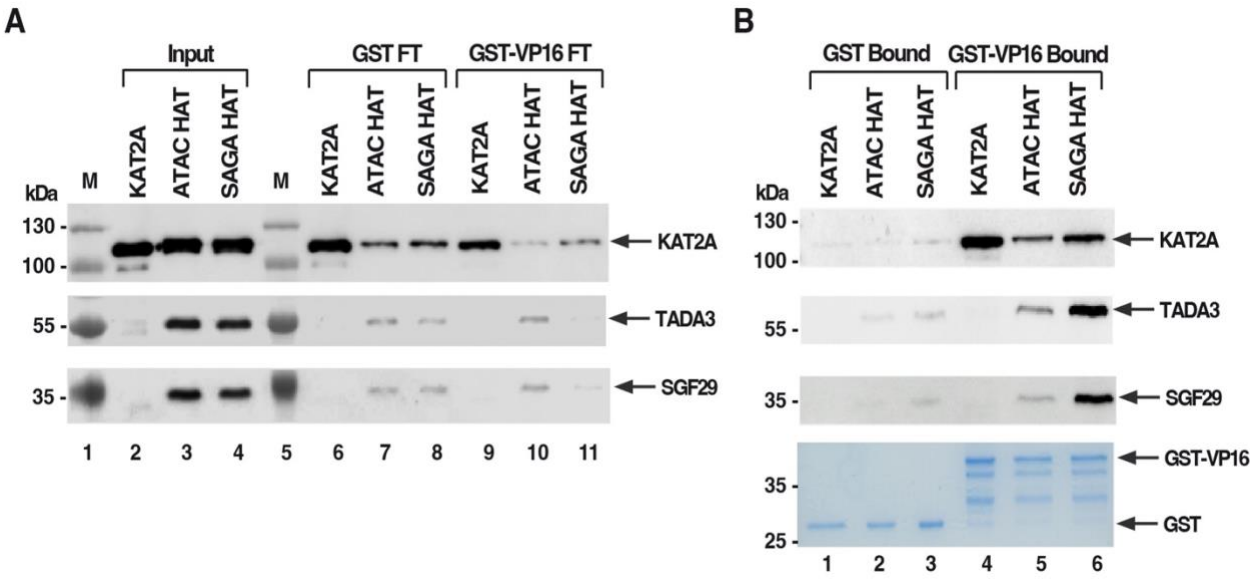

Figure S5. Binding of recombinant KAT2A, $SAGA_{HAT}$ or $ATAC_{HAT}$ to VP16-AD. (A) Western blots of input (0.1 %) purified KAT2A, $ATAC_{HAT}$, and $SAGA_{HAT}$ fractions (lane 2, 3 and 4). KAT2A, $ATAC_{HAT}$, and $SAGA_{HAT}$ GST flow through (FT) (0.1%) (lane 6, 7 and 8) and GST-VP16 FT (0.1%) (lane 9, 10 and 11). (B) Purified KAT2A, $ATAC_{HAT}$, and $SAGA_{HAT}$ fractions were incubated with either GST (lane 1, 2, and 3) or GST-VP16 (lane 4, 5, and 6) columns, washed and eluted. Elutions (~14%) were resolved by SDS-PAGE and analyzed by Western blot with the indicated antibodies. Equal loading was tested by Coomassie brilliant blue staining of either GST (lane 1, 2, and 3) or GST-VP16 (lane 4, 5, and 6) protein containing beads. Each binding measurement was repeated in triplicate.

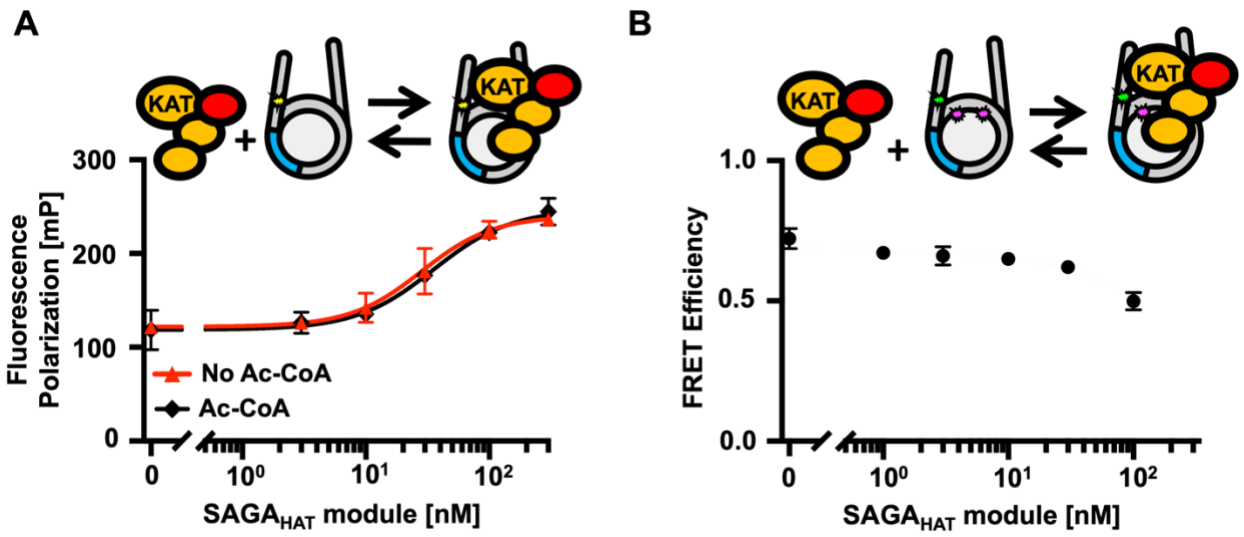

Figure S6. $SAGA_{HAT}$ interactions with nucleosomes. (A) Fluorescence Polarization in mP of nucleosomes with increasing amounts of the $SAGA_{HAT}$ module. The $SAGA_{HAT}$ module binds with an S1/2 of 25.0 ± 0.3 nM (red triangle) and reaches saturating conditions around 100 nM. The $SAGA_{HAT}$ module with Ac-CoA binds at a S1/2 of 37 ± 3 nM. (B) FRET of the $SAGA_{HAT}$ module binding nucleosomes at increasing amounts. Each FRET and fluorescence polarization value was determined in triplicate and the uncertainty was determined from the standard error of the three measurements.

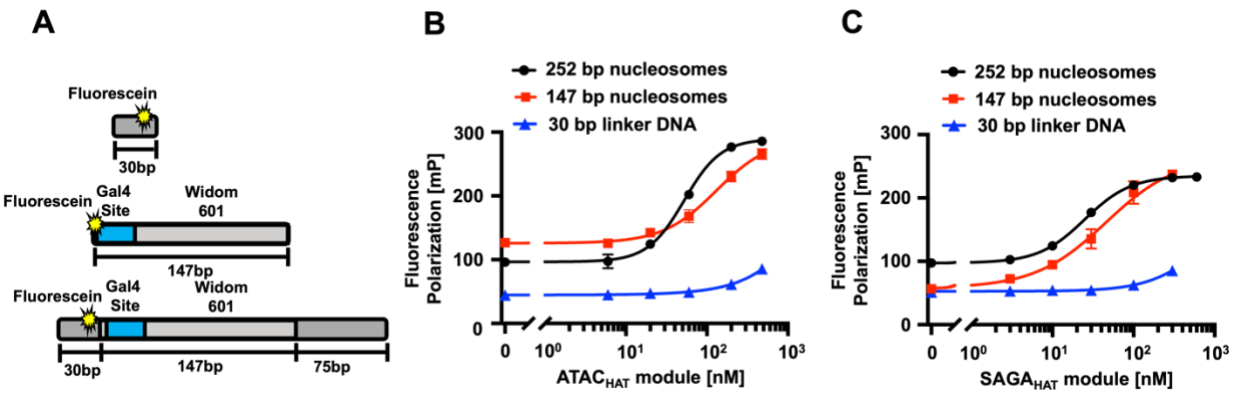

Figure S7. $ATAC_{HAT}$ and $SAGA_{HAT}$ interactions with nucleosomes and linker DNA. (A) DNA constructs for fluorescence polarization measures of $ATAC_{HAT}$ and $SAGA_{HAT}$ binding to 30 bp DNA, nucleosomes without linker DNA (147 bp DNA) and nucleosomes with linker DNA (252 bp DNA). (B and C). Fluorescence Polarization (mP) of nucleosomes with increasing amounts of either the $ATAC_{HAT}$ or $SAGA_{HAT}$ module. (B) The $ATAC_{HAT}$ module binds to 252 bp nucleosomes with a S1/2 of 50 ± 2 (black circle), 147 bp nucleosomes with a S1/2 of 130 ± 30 nM (red square), and to the 30 bp linker DNA with a S1/2 over 500 nM (blue triangle). (C) The $SAGA_{HAT}$ module binds to 252 bp nucleosomes with a S1/2 of 25.0 ± 0.3 (black circle), 147bp nucleosomes with a S1/2 of 46 ± 10 nM (red square), and to the 30 bp linker DNA with a S1/2 over 300 nM (blue triangle). Each fluorescence polarization value was determined in triplicate and the uncertainty was determined from the standard error of the three measurements.

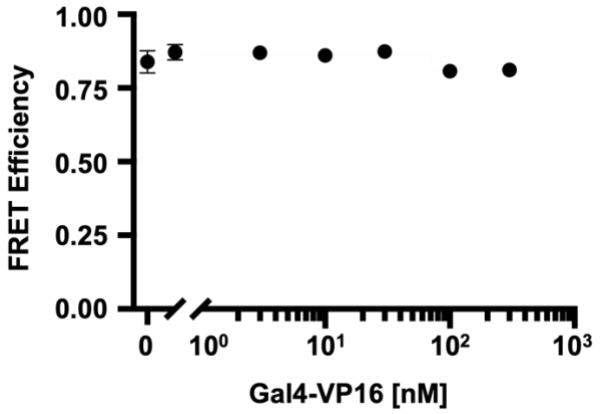

Figure S8. Measuring Gal4 site specificity within nucleosomes. Titrating Gal4-VP16 while measuring FRET efficiency to nucleosomes that do not contain a Gal4 binding site. This experiment shows that the Gal4 binding site is required for Gal4-induced nucleosome unwrapping. Each FRET value was determined in triplicate and the uncertainty was determined from the standard error of the three measurements.

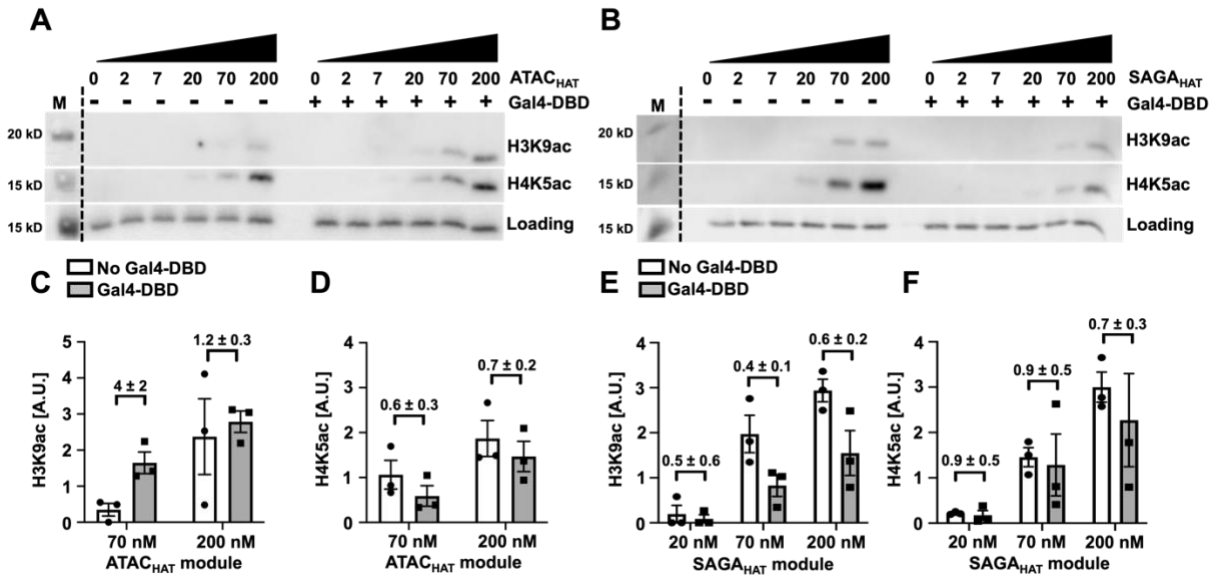

Figure S9: Influence of the of Gal4-DBD on the acetylation by the ATAC and SAGA HAT modules. Acetylation assay by the $ATAC_{HAT}$ (A) or $SAGA_{HAT}$ (B) modules at increasing concentrations with and without Gal4-DBD at the indicated PTM sites. The fluorescence of Cy5-labeled histone H2A within the nucleosome was used to observe nucleosome loading. Acetylation efficiency was tested by Western blot using antibodies recognizing either histone H3K9ac or H4K5ac. Images are representative of three independent experiments with similar results ($n = 3$). Two-tailed, unpaired t-test with Welch's correction was conducted using Prism 9 software. Error bars represent standard error of the mean. (C, D) Bar plots of A (E, F) Bar plots of B.

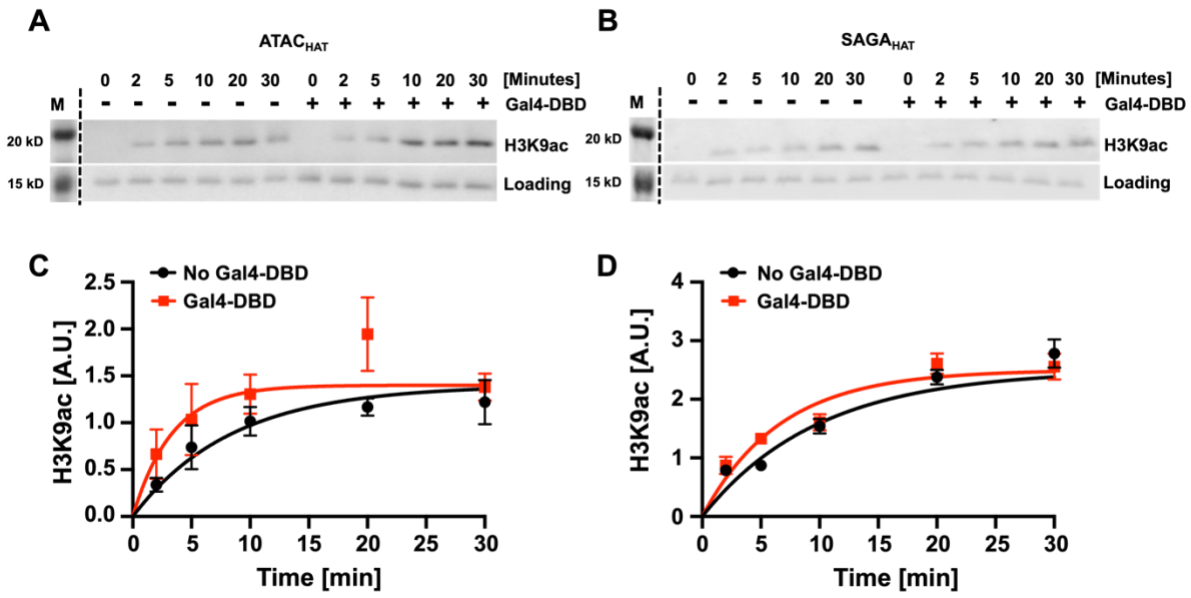

Figure S10: The acetylation kinetics of nucleosomes at H3K9 by ATAC$_{HAT}$ and SAGA$_{HAT}$. Acetylation assay by the ATAC$_{HAT}$ (A) or SAGA$_{HAT}$ (B) module at increasing time with and without Gal4-DBD at H3K9ac. The fluorescence of Cy5-labeled histone H2A within the nucleosome was used to observe nucleosome loading. Acetylation efficiency was tested by Western blot using antibodies recognizing histone H3K9ac. Images are representative of three independent experiments with similar results ($n = 3$). Error bars represent standard error of the mean. (C) Graphs of A (D) Graph of B. The time courses were fit to a single exponential as described in the Methods section.

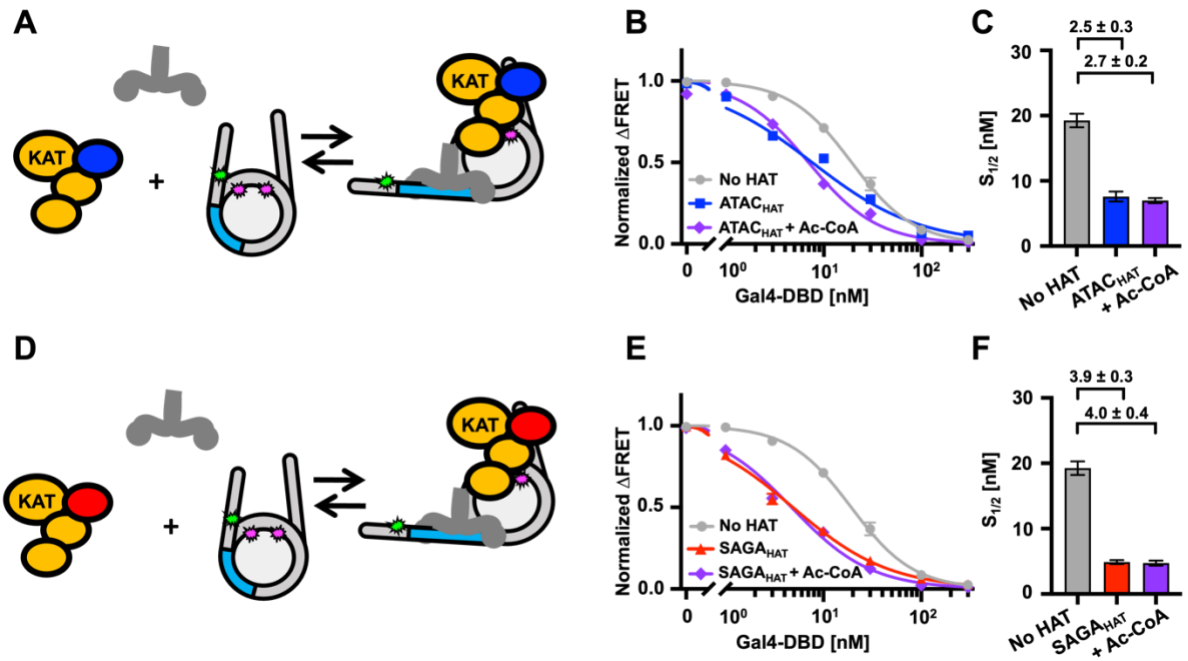

Figure S11: ATAC$_{HAT}$ and SAGA$_{HAT}$ influence nucleosome accessibility of Gal4-DBD binding independent of Ac-CoA. (A) Binding model of Gal4-DBD and the ATAC$_{HAT}$ module binding to a nucleosome. (B) Normalized ΔFRET of Gal4-DBD binding nucleosomes with increasing amounts. Gal4-DBD binding to nucleosomes at a $S_{1/2}$ of 19 ± 1 nM (light gray circles), Gal4-DBD binding to nucleosomes with the addition of 200 nM ATAC$_{HAT}$ at a $S_{1/2}$ of 7.6 ± 0.8 nM (dark blue squares), and with the addition of 30 μM Ac-CoA at a $S_{1/2}$ of 7.0 ± 0.4 nM (purple diamond). (C) Bar plot of S1/2 values from B (D) Binding model of Gal4-DBD and the SAGA$_{HAT}$ module binding to a nucleosome. (E) Normalized ΔFRET of Gal4-DBD binding to nucleosomes at increasing amounts. Gal4-DBD binding to nucleosomes at a $S_{1/2}$ of 19 ± 2 nM (light gray circles), Gal4-DBD binding to nucleosomes with the addition of 150 nM SAGA$_{HAT}$ at a $S_{1/2}$ of 4.9 ± 0.3 nM (red triangles), and with the addition of 30 μM Ac-CoA at a $S_{1/2}$ of 4.7 ± 0.4 nM (purple diamond). (F) Bar plot of $S_{1/2}$ and standard error values from the weighted fits to binding isotherms in E. Each FRET value was determined in triplicate and the uncertainty is determined from the standard error of the three measurements. The $S_{1/2}$ values were determined from a weighted fit of the titration to a binding isotherm and the uncertainty was determined from the covariance matrix of the weighted fit.

Supplemental Tables

Binding Target	HAT Module	Ac-CoA	$S_{1/2}$ (nM)	P value	P < 0.2
252 bp nucleosomes	ATAC HAT	No	50 ± 2	n/a	n/a
252 bp nucleosomes	ATAC HAT	Yes	40 ± 1	0.02	yes
252 bp nucleosomes	SAGA HAT	No	25.0 ± 0.3	n/a	n/a
252 bp nucleosomes	SAGA HAT	Yes	37 ± 3	0.06	yes
147 bp nucleosomes	ATAC HAT	No	130 ± 30	0.12	yes
147 bp nucleosomes	SAGA HAT	No	50 ± 10	0.13	yes
30 bp DNA	ATAC HAT	No	> 500	n/a	n/a
30 bp DNA	SAGA HAT	No	> 300	n/a	n/a

Table S1. Fluorescence polarization fit values. The $S_{1/2}$ values were determined from weighted fits if the HAT module titrations to binding isotherms. The uncertainty was determined from the covariance matrix of the weighted fit. P values for the 252 nucleosomes with Ac-CoA to 252 nucleosomes without Ac-CoA. The P values for 147 bp nucleosomes is in comparison to 252 bp nucleosomes.

HAT (nM)	TF	PTM	Blot Signal	Ratio	P value	P < 0.2
ATAC (70 nM)	+ Gal4-VP16	H3K9ac	0.7 ± 0.1	5 ± 2	0.01	yes
	- Gal4-VP16	H3K9ac	0.15 ± 0.05			
ATAC (200 nM)	+ Gal4-VP16	H3K9ac	2.0 ± 0.2	1.0 ± 0.2	1.00	n.s.
	- Gal4-VP16	H3K9ac	2.0 ± 0.3			
ATAC (70 nM)	+ Gal4-VP16	H4K5ac	0.7 ± 0.4	6 ± 5	0.28	n.s.
	- Gal4-VP16	H4K5ac	0.11 ± .06			
ATAC (200 nM)	+ Gal4-VP16	H4K5ac	2.2 ± 0.5	1.0 ± 0.3	0.91	n.s.
	- Gal4-VP16	H4K5ac	2.3 ± 0.5			
SAGA (20 nM)	+ Gal4-VP16	H3K9ac	1.0 ± 0.3	3 ± 1	0.10	yes
	- Gal4-VP16	H3K9ac	0.3 ± 0.1			
SAGA (70 nM)	+ Gal4-VP16	H3K9ac	2.7 ± 0.8	1.8 ± 0.6	0.30	n.s.
	- Gal4-VP16	H3K9ac	1.5 ± 0.3			
SAGA (200 nM)	+ Gal4-VP16	H3K9ac	3 ± 1	1.7 ± 0.6	0.38	n.s.
	- Gal4-VP16	H3K9ac	1.8 ± 0.3			
SAGA (20 nM)	+ Gal4-VP16	H4K5ac	0.25 ± 0.03	2.5 ± 2.5	0.37	n.s.
	- Gal4-VP16	H4K5ac	0.1 ± 0.1			
SAGA (70 nM)	+ Gal4-VP16	H4K5ac	2.0 ± 0.3	2.2 ± 0.4	0.11	yes
	- Gal4-VP16	H4K5ac	0.9 ± 0.08			
SAGA (200 nM)	+ Gal4-VP16	H4K5ac	2.9 ± 0.8	1.3 ± 0.5	0.49	n.s.
	- Gal4-VP16	H4K5ac	2.2 ± 0.6			

Table S2. Summary of $ATAC_{HAT}$ and $SAGA_{HAT}$ Western blot analysis with Gal4-VP16. Each blot signal is the average of at least three measurements. The uncertainty is determined from the standard error.

HAT Module	TF	τ_{noTF} (sec)	τ_{TF} (sec)	τ_{noTF} / τ_{TF}
ATAC	Gal4-VP16	60 ± 10	13.0 ± 0.5	4.6 ± 0.2
SAGA	Gal4-VP16	40 ± 4	7.8 ± 0.2	5.1 ± 0.1
ATAC	Gal4-DBD	8 ± 1	3 ± 1	2.7 ± 0.4
SAGA	Gal4-DBD	10 ± 2	6.6 ± 0.3	1.5 ± 0.2

Table S3. Summary of $ATAC_{HAT}$ and $SAGA_{HAT}$ time course Western blot analysis with Gal4-VP16 and Gal4-DBD. The time courses were determined from the weighed fit with a single exponential as described in the Methods section to determine characteristic time, τ, for the acetylation reaction. The uncertainties were determined from the covariance matrix of the weighted fit.

HAT (nM)	TF	PTM	Blot Signal	Ratio	P value	P < 0.2
ATAC (70 nM)	+ Gal4-DBD	H3K9ac	1.7 ± 0.3	4 ± 2	0.03	yes
	- Gal4-DBD	H3K9ac	0.4 ± 0.2			
ATAC (200 nM)	+ Gal4-DBD	H3K9ac	2.8 ± 0.3	1.2 ± 0.3	0.74	n.s.
	- Gal4-DBD	H3K9ac	2.4 ± 0.6			
ATAC (70 nM)	+ Gal4-DBD	H4K5ac	0.6 ± 0.3	0.6 ± 0.3	0.30	n.s.
	- Gal4-DBD	H4K5ac	1.06 ± .08			
ATAC (200 nM)	+ Gal4-DBD	H4K5ac	1.9 ± 0.6	0.7 ± 0.2	0.49	n.s.
	- Gal4-DBD	H4K5ac	2.8 ± 0.3			
SAGA (20 nM)	+ Gal4-DBD	H3K9ac	0.09 ± 0.09	0.5 ± 0.6	0.66	n.s.
	- Gal4-DBD	H3K9ac	0.2 ± 0.2			
SAGA (70 nM)	+ Gal4-DBD	H3K9ac	0.8 ± 0.2	0.4 ± 0.1	0.09	yes
	- Gal4-DBD	H3K9ac	2.0 ± 0.4			
SAGA (200 nM)	+ Gal4-DBD	H3K9ac	1.6 ± 0.5	0.6 ± 0.2	0.09	yes
	- Gal4-DBD	H3K9ac	2.9 ± 0.3			
SAGA (20 nM)	+ Gal4-DBD	H4K5ac	0.2 ± 0.1	0.9 ± 0.5	0.70	n.s.
	- Gal4-DBD	H4K5ac	0.22 ± 0.02			
SAGA (70 nM)	+ Gal4-DBD	H4K5ac	1.3 ± 0.7	0.9 ± 0.5	0.83	n.s.
	- Gal4-DBD	H4K5ac	1.5 ± 0.2			
SAGA (200 nM)	+ Gal4-DBD	H4K5ac	2 ± 1	0.7 ± 0.3	0.56	n.s.
	- Gal4-DBD	H4K5ac	3.0 ± 0.3			

Table S4. Summary of $ATAC_{HAT}$ and $SAGA_{HAT}$ Western blot analysis with Gal4-DBD. Each blot signal is the average of at least three measurements. The uncertainty is determined from the standard error.

TF	HAT Module	Ac-CoA	$S_{1/2}$ (nM)	$S_{1/2\ noHAT}$ / $S_{1/2\ HAT}$	P value
Gal4-VP16	None	-	55 ± 2	N.A.	N.A.
Gal4-VP16	ATAC	-	5.3 ± 0.7	10 ± 1	0.0006
Gal4-VP16	ATAC	+	7 ± 1	8 ± 1	0.0003
Gal4-VP16	SAGA	-	7 ± 1	8 ± 1	0.0003
Gal4-VP16	SAGA	+	6.5 ± 0.9	8 ± 1	0.0003
Gal4-DBD	None	-	19 ± 1	N.A.	N.A.
Gal4-DBD	ATAC	-	7.6 ± 0.8	2.5 ± 0.3	0.001
Gal4-DBD	ATAC	+	7.0 ± 0.4	2.7 ± 0.2	0.003
Gal4-DBD	SAGA	-	4.9 ± 0.3	3.9 ± 0.3	0.003
Gal4-DBD	SAGA	+	4.7 ± 0.4	4.0 ± 0.4	0.002

Table S5. Measurement values of transcription factor $S_{1/2}$ with HAT modules. The $S_{1/2}$ values were determined from weighted fits of the HAT module titrations to binding isotherms. The uncertainty was determined from the covariance matrix of the weighted fit.